

# Structure and Infrastructure Engineering

## Maintenance, Management, Life-Cycle Design and Performance

ISSN: (Print) (Online) Journal homepage: <https://www.tandfonline.com/loi/nsie20>

## Parametric analysis of the dynamic response of railway bridges due to vibrations induced by heavy-haul trains

Emrah Erduran, Semih Gonen & Aya Alkanany

To cite this article: Emrah Erduran, Semih Gonen & Aya Alkanany (2022): Parametric analysis of the dynamic response of railway bridges due to vibrations induced by heavy-haul trains, Structure and Infrastructure Engineering, DOI: [10.1080/15732479.2022.2090582](https://doi.org/10.1080/15732479.2022.2090582)

To link to this article: <https://doi.org/10.1080/15732479.2022.2090582>



© 2022 The Author(s). Published by Informa UK Limited, trading as Taylor & Francis Group



Published online: 26 Jun 2022.



Submit your article to this journal [↗](#)




View related articles [↗](#)



View Crossmark data [↗](#)

# Parametric analysis of the dynamic response of railway bridges due to vibrations induced by heavy-haul trains

Emrah Erduran , Semih Gonen  and Aya Alkanany

Department of Civil Engineering and Energy Technology, Oslo Metropolitan University, Oslo, Norway

## ABSTRACT

This article presents a numerical study that aims to explore the dynamic behavior of railway bridges under vibrations induced by heavy-haul traffic. For this purpose, a finite element code that can conduct moving load and moving mass analysis of single span bridges was developed. The software was validated by comparing the numerical response to the analytical solution for various speeds. The numerical analysis of the benchmark bridge under the benchmark train showed the interplay between the natural frequency of the bridge, the mass of the train and the loading frequency. A comprehensive parametric study to investigate the impact of different parameters on the dynamic behavior of railway bridges is also provided. The bridge span length, normalized train length, normalized mass of the train, bridge deck stiffness, and train speed are the variables considered in the parametric study. The results of the extensive numerical analyses improve the understanding of railway bridge behavior under heavy-haul trains, and highlight the impact of the inertial effect of the trains on bridges, especially for varying span length and deck stiffness. It is also demonstrated that, when the train-to-bridge mass ratio exceeds 40%, the inertial effects of the train mass needs to be included in the analysis in order to obtain a reliable estimate of the bridge behavior under different train speeds.

## ARTICLE HISTORY

Received 4 February 2022  
Accepted 6 May 2022

## KEYWORDS

Railway bridges; resonance; critical speed; moving mass; moving load; heavy-haul trains; acceleration response

## 1. Introduction

The rapid increase in societal development leads to a demand for more goods to be transported over longer distances at higher speeds than ever before. In this regard, heavy-haul freight railways offer exceptionally efficient long-distance transportation of goods that is both economically attractive and has a very low environmental footprint compared to other transportation modes. The advancements in the train technology enables the trains to meet the increasing demands in capacity and speed due to societal changes. On the other hand, the aging bridge infrastructure cannot match the rapid advancement in the train technology and the increase in demands. As of 2017, more than 35% of half a million railway bridges in Europe are over 100 years old, with many more on the wrong side of their 50-year design life (Casas and Moughty (2017)). Therefore, the existing bridge infrastructure, which has been designed for smaller traffic loads, remains a potential bottleneck for increased axle loads and speed of heavy-haul freight trains.

The safety of the railway bridges is mainly governed by their dynamic response and fatigue life. Under heavy-haul freight train loading, both the dynamic response and the fatigue life can be influenced significantly by the train-induced vibrations. Unlike random loading on highway bridges, the train loading on railway bridges has a specific frequency spectrum that can significantly impact the bridge's behavior. This

interaction has been studied extensively using a number of approaches of different complexities over the last decades especially after the introduction of high-speed trains; e.g. Frýba (1999); Ichikawa et al. (2000); Michaltsos et al. (1996).

Garinei and Risitano (2008) investigated the behavior of simply-supported short- and medium-span bridges considering the constant and harmonic components of the train loading. Xia et al. (2006) analyzed various types of resonance mechanisms of the train-bridge system. Similarly, Yang et al. (2004) studied the mechanisms of resonance and cancellation for the bridges resting on elastic bearings. On the other hand, Yang and Lin (2005) investigated the frequency aspects of the dynamic interaction between the train and simply supported bridges, where the train-to-bridge mass ratio is assumed to be small. Similarly, Lu et al. (2012) investigated the frequency characteristics of bridge response, whereas Jin et al. (2017) derived a frequency domain solution to the bridge vibration problem. Common to these studies is the relative simplicity of the train and bridge models used.

More complex models such as multi-body vehicle systems were also used in many cases. Cheng et al. (2001) used a bridge-track-vehicle element which consists of vehicles modeled as mass-spring-damper systems and beam elements to model the rails and the bridge deck. They found that the effect of track structure on the dynamic response of bridge structure is negligible. Kwark et al. (2004) idealized the

problem and compared their solution to the moving load method numerically and using field tests. Majka and Hartnett (2008) also utilized different modeling approaches to carry out a parametric analysis. In their study, vehicle damping was found to have a negligible influence on the bridge response. Xia and Zhang (2005) analyzed the dynamic behavior of a railway bridge and compared the results to the field measurements.

In another aspect, Ju and Lin (2003) and Ju et al. (2009) investigated the vibration characteristics of the bridge-train system using a complex numerical model and field tests. Arguably, the most detailed parametric studies on this topic were reported by Arvidsson and Karoumi (2014) and Doménech et al. (2014). In both studies, the train-bridge interaction was modeled using both simple moving load models and more detailed interaction models. Impact of several parameters on the reduction in acceleration demands using detailed train bridge interaction models were evaluated and discussed. These studies, similar to most of the others found in literature focused on high-speed trains, e.g. Garinei and Risitano (2008); Ju and Lin (2003); Ju et al. (2009); Kwark et al. (2004); Liu et al. (2009); Xia and Zhang (2005), which, in general have a relatively low mass that can be assumed to be negligible compared to the mass of the bridge. While this assumption should be expected to be valid for most of the trains including the high-speed passenger trains, the train mass can become significant as compared to the bridge mass for heavy-haul freight trains, which are generally characterized by an axle load of 250 to 350 kN.

Only a few studies have been conducted on the interaction between railway bridges and heavy-haul trains. Zhu et al. (2018) employed pseudo-excitation method to investigate the effects of train speed and track irregularity on the dynamic behavior of the bridges carrying heavy-haul trains. Xiao et al. (2020) used a multi-body vehicle model to investigate the dynamic behavior of bridges under freight train loading in China. In both studies, track irregularities were taken into account, and bridge response with changing train speeds is obtained. However, the characteristics of bridge vibrations and several parameters affecting the bridge response were not investigated. Due to the significant mass of the trains relative to the bridge mass and the considerable length of freight trains, heavy-haul train-induced bridge vibrations are of particular interest to the safety of the existing bridge infrastructure. Indeed, the need for further research on this topic was highlighted in a recent review article (Arvidsson and Karoumi (2014)), where the train-bridge interaction problem and key model parameters were discussed. Further, very few works focused on systematically quantifying the impact of the train mass on the bridge behavior to develop guidelines and recommendations for practical applications.

This article contributes to the understanding of the dynamic behavior of railway bridges under vibrations induced by heavy-haul trains by systematically investigating the interplay between the frequency characteristics of the loading, the train mass, the natural vibration frequency of the bridge, and the dynamic bridge response. It also provides a comprehensive parametric study to explain the effects of key parameters

of heavy-haul train-induced vibrations on the bridge response, which is currently missing in the literature. Although a number of studies investigated the effects of different parameters on the dynamic behavior of railway bridges, none of the existing studies, to the best of our knowledge, considered all the parameters investigated in this study concurrently and, thus, were more limited in their scope. Furthermore, existing studies presented herein employed a much smaller mass compared to the existing heavy-haul trains, which did not generally impact the vibration frequencies of the bridge. This study explores the interaction between the heavy-haul trains and bridges and the capability of moving load and moving mass in capturing this interaction. In addition, this study displays the variation of the resonance behavior under multiple variables and demonstrates the practical implications of including or ignoring the train mass in the numerical analysis in terms of the critical train speed and amplified acceleration response.

The article is structured in the following way: the Finite Element code generated to analyze the dynamic behavior of bridges is summarized. A simply-supported, 50 m long prestressed concrete railway bridge was selected as the benchmark case and introduced next. Results of the analysis obtained using the developed code are compared to dynamic in-situ measurements for model verification. Afterward, the resonance characteristics of the benchmark bridge and the iron ore trains are studied, focusing on the impact of the train mass on these characteristics. A parametric study that includes the bridge span length, length of the train normalized by the span length, the normalized mass of the train, bridge deck stiffness, and the train's speed is conducted to study the impact of these parameters on the resonant vibration characteristics and the dynamic response of the railway bridges. Finally, the conclusions drawn from the conducted analysis are summarized and needs for future research is discussed.

## 2. Train model

Trains can be modeled using three approaches: (1) as a Moving Load (ML) model where the train is modeled as a series of rolling loads and inertial effect, stiffness, and the damping properties of the vehicle are ignored, (2) as a Moving Mass (MM) model where the inertial effect of the vehicle is included by modeling the train as a series of rolling masses while the stiffness and the damping of the vehicle are ignored, (3) the vehicle is modeled using an advanced approach where springs, dashpots, and masses are used to simulate the stiffness, damping and inertial effects of the vehicles, respectively. As summarized in Karoumi (1998), Yang et al. (2004), and Wiberg (2009), the most complex train model, *i.e.*, the mass-spring-dashpot model, is required only for special cases. For example, when the acceleration levels of the trains need to be checked or for bridges where the dynamic impacts are mainly caused by the roughness of the rail surface and not by the vibrations of the bridge itself. Since the focus of this study is to investigate the dynamic behavior of the bridge due to the elastic displacement of the bridge itself, the first two models were

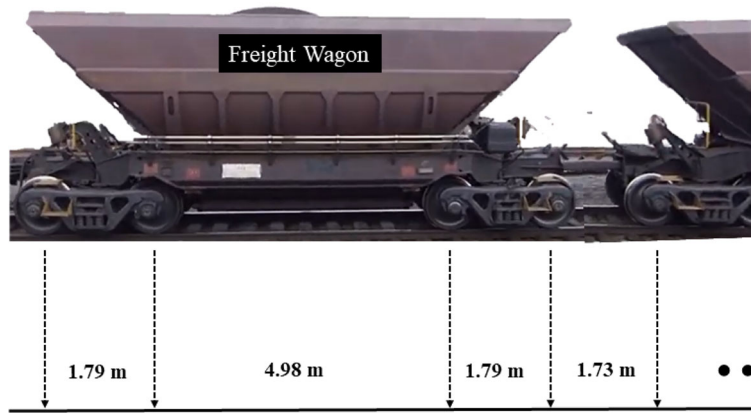


Figure 1. Freight wagons used in transferring iron ore on the Ofot line and their axle spacing.

used in the study, ignoring the stiffness and damping properties of the vehicle.

The track irregularities are not considered in the moving mass model because the main focus of the article is to evaluate and compare the frequency content of the bridge vibrations generated by moving load and moving mass models. Although the amplitudes of vibrations are used in the article to identify the resonance conditions and the critical speeds, prediction of the acceleration amplitudes is out of the scope of this article. For this reason, only the vibrations that are created by the bending behavior of the bridge is considered and not by other sources such as track irregularities, which do not impact the resonance frequencies and critical speeds. Therefore, neglecting the track irregularities does not have a significant impact on the results of the study. This approach is in line with previous work that has a similar focus with this article and also did not consider the track irregularities (Arvidsson and Karoumi (2014); Cheng et al. (2001); Doménech et al. (2014); Kwark et al. (2004)). Effect of track irregularities on the amplitudes of accelerations are reported elsewhere; see Jin et al. (2017); Ju and Lin (2003); Ju et al. (2009); Xia and Zhang (2005); Xia et al. (2005); Xiao et al. (2020).

The benchmark train used in the study is an iron ore freight train used on the Ofot line in to haul the iron ore mined in Kiruna, Sweden to the harbor in Narvik, Norway. The train consists of 68 iron ore wagons, each with four axles resulting in a total of 272 axles distributed over a total length of approximately 700 meters. In this study, an axle load of 325 kN is used, resulting in a total train mass of 8840 tons. Figure 1 shows the overview of the axle configuration and an example of the iron ore wagons.

To explore the frequency content of the dynamic loading induced by the benchmark train, the time history of the wheel loading of the benchmark train passing a given point on the bridge is formulated as (Ju et al. (2009)):

$$P(t) = \sum_{j=1}^{N_c} \sum_{k=1}^{N_w} (P_{axle}(\delta(t - t_k - jt_c))) \quad (1)$$

where  $N_c$  and  $N_w$  are the number of carriages and pairs of wheels in a unit carriage, respectively, and  $P_{axle}$  is the axle load. The moment in time that the  $k^{th}$  wheel passes the

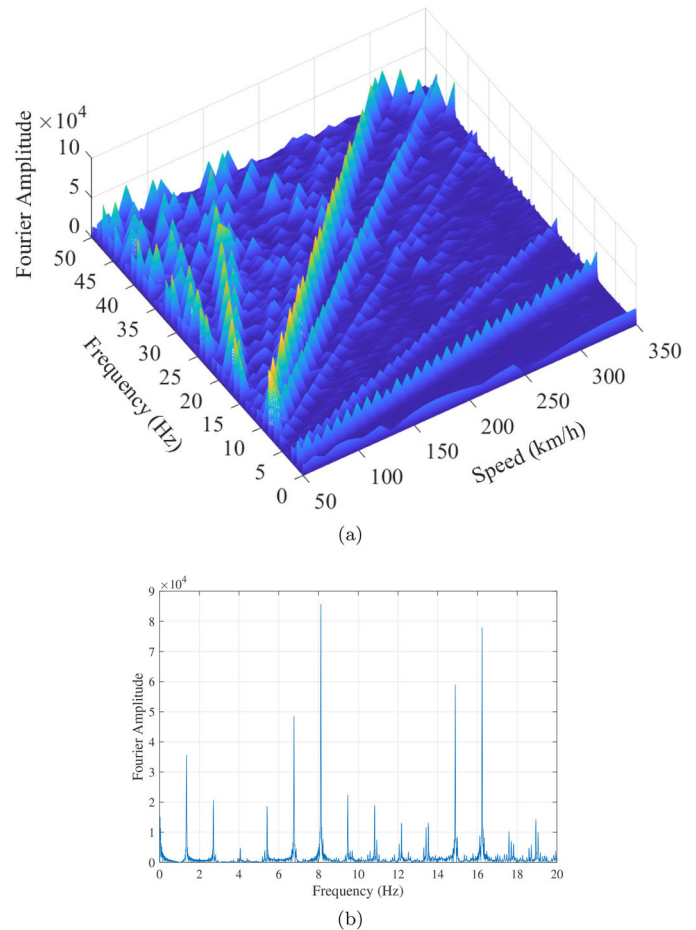


Figure 2. FAS of loading for (a)  $V = 50\text{--}350$  km/h, (b)  $V = 50$  km/h.

given point is designated by  $t_k$ , while  $t_c$  represents the time a carriage completely passes the point and can be computed as  $t_c = L/V$  in which  $V$  is the train speed and  $L$  is the distance between the centers of two consecutive carriages.

The function of the train load is then converted to the frequency domain via Fourier transform using the approach summarized in Ju et al. (2009). Dominant frequencies of the loading then is given by:

$$f = nV/L \quad (2)$$

where  $n$  is a positive integer. Figure 2(a) shows the frequency spectra of the train loading for the speed range of

50 km/h to 350 km/h. The dominant frequencies of the train loading increase linearly with the increasing train speed, as seen in Figure 2(a) and can be deduced from Equation (2). These linear peaks spreading out from the origin to the edges of the figure are associated with the different values of the integer  $n$  in Equation (2). Also plotted in Figure 2(b) is the frequency spectrum of the train loading at a speed of 50 km/h, which is the specified traveling speed of the benchmark train on the benchmark bridge. This figure more clearly depicts the predominant frequencies of the loading at a speed 50 km/h at different frequencies of  $n$  starting with  $f=1.35$  for  $n=1$ .

### 3. Benchmark bridge and impact of mass of the benchmark train on the frequency characteristics of the bridge

Norrdals bridge, a prestressed concrete, single-span bridge with a span length of 50 m, was used as the benchmark bridge in the study. The bridge deck has a double-tee cross-section with a total depth of 2.85 m. It is 6.6 m wide and houses a single, ballasted track. The area and the moment of inertia of its cross-section are  $6.81 \text{ m}^2$  and  $16.89 \text{ m}^4$ , respectively. The longitudinal axis of the bridge is straight with no curvature.

In this study, normalized train mass is defined as the ratio of the maximum train mass that can be on the bridge at a given time to the mass of the bridge. The total mass of the bridge is computed as 867.8 tons. At a given instant, out of the total 272 axles of the benchmark train, a maximum of 20 axles can be on the bridge. With an axle load of 325 kN, the maximum train mass that is on the bridge at a given time can then be computed as 662.6 tons. Dividing this value by the total mass of the bridge leads to a normalized train mass of 0.76 for the benchmark train and the benchmark bridge.

The accelerations on the benchmark bridge were monitored for 24 hours in August 2020 in order to understand the vibration characteristics of the bridge. The instrumentation deployed on the bridge consists of 20-bit low noise low-power, triaxial MEMS digital accelerometers. A total of five accelerometers were deployed on the bridge. Details of the measurement campaign and the identified vibration characteristics of the bridge under both ambient and train-induced vibrations is reported in Salehi et al. (2021).

Accelerations induced by both the benchmark train and lightweight maintenance trains that consists of a single locomotive were recorded during the measurement campaign. To quantify the effect of the mass of the benchmark train on the vibration frequency of the bridge, Fourier Amplitude Spectrum of the accelerations induced by the benchmark and lightweight trains are plotted in Figure 3. While the benchmark train increases the total mass of the bridge by 76%, the mass of the lightweight train is negligible compared to the mass of the bridge. As such, the vibrations induced by the lightweight train occur at the fundamental vibration frequency of the bridge itself. On the other hand, the mass of the benchmark train, significantly impacts the

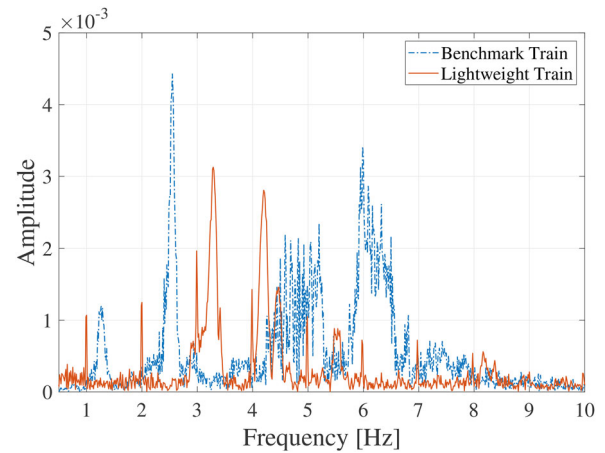


Figure 3. Fourier Amplitude Spectrum of the accelerations recorded at the mid-span.

vibration frequencies of the bridge leading to a 20% decrease in the fundamental vibration frequency.

This observed variation in the vibration frequency due to the mass of the train differs significantly from the results reported in the literature that mainly focuses on the train-bridge interaction for high-speed passenger trains (e.g. Arvidsson and Karoumi (2014); (2014); Liu et al. (2009)), which have a much smaller mass compared to the heavy-haul trains and does not generally impact the vibration frequencies of the bridge. Motivated by this observation, the following sections explore the interaction between the heavy-haul trains and bridges and the capability of moving load and moving mass in capturing this interaction.

### 4. Finite element model & verification

In order to numerically obtain the displacement and acceleration responses of a simply supported bridge under moving loads and moving mass, a Finite Element code is generated. Several commercial packages such as ABAQUS and ANSYS are capable of conducting moving load and moving mass analysis, albeit at a relatively high computational cost. It was decided to develop a new FE code in MATLAB computational environment due to the sheer number of numerical analysis carried out to conduct the parametric investigated reported in this article. In total, 11840 time-history analyses were conducted by varying different key bridge and train parameters, which required a robust code that can be run automatically and efficiently. As such, a FE code written in MATLAB is preferred over commercially available software.

In the developed FE code, the bridge deck is modeled using Bernoulli beam-column line elements discretized by nodes spaced at regular intervals. At each node, three degrees of freedom, translations in the longitudinal and vertical direction and rotation about the transverse axis, were considered. The stiffness matrix of each element is constructed using Euler-Bernoulli formulation, while the mass matrix is developed using the consistent mass matrix for an Euler-Bernoulli beam associated with the translational inertia (Fryba (1999)). The mass matrix is based solely on the bridge mass for the moving load model and remains

constant throughout the analysis. On the other hand, for the moving mass model, the mass matrix is updated at each time step to account for the train mass on the bridge at that time step. The equation of motion is solved using a linear solver based on Newmark's direct integration method. The developed software can compute the acceleration, velocity, and displacement at each node for the moving load and moving mass models.

The developed FE software is validated by computing the displacement response of an undamped simply-supported beam under a single moving mass using the developed software and the results are compared with the analytical solution presented in Michaltsos et al. (1996) as summarized in the following paragraphs.

A mathematical formulation to obtain the displacement response of a simply supported beam under a moving mass is briefly described in the following. The beam has a length  $L$ , mass per unit length  $\rho$  and flexural rigidity  $EI$ . A mass,  $M$ , moving with a constant velocity,  $V$ , exerts a force,  $P$ , on the beam:

$$P = Mg - M\ddot{u}(Vt) \quad (3)$$

where  $g$  represents the acceleration of gravity,  $u$  is the vertical displacement, and  $t$  is the time. Using the elastic beam theory, the equation of motion can be written as:

$$EIu''''(x, t) + m\ddot{u}(x, t) = Mg\delta(x - Vt) - M\ddot{u}\delta(x - Vt) \quad (4)$$

where the *prime* denotes differentiation with respect to  $x$ , *dot* represents differentiation with respect to  $t$  and  $\delta$  is the Dirac delta function.

Using modal analysis approach, the vertical displacement can be expressed as:

$$u(x, t) = \sum_n \phi_n(x)q_n(t) \quad (5)$$

where  $\phi_n$  are the mode shapes of the beam and  $q_n(t)$  are the modal amplitudes to be computed. Inserting Equation (5) in Equation (4):

$$\begin{aligned} EIu(x, t) \sum_n \phi_n(x)''''q_n(t) + m \sum_n \phi_n(x)\ddot{q}_n(t) \\ = Mg\delta(x - Vt) - M \sum_n \phi_n(x)\ddot{q}_n(t)\delta(x - Vt) \end{aligned} \quad (6)$$

For a simply supported beam, the mode shapes can be written as the shape functions of a freely vibrating beam;  $\phi_n = \sin(n\pi x/L)$ . The modal amplitudes and the displacement response can then be solved analytically using the approach summarized in Michaltsos et al. (1996).

In Figure 4, the displacement response of the middle of the simply supported beam exposed to a single moving load and moving mass models are investigated by running both models for train speeds varying from 50 km/h to 350 km/h. Figure 5 shows the Fourier amplitude spectra of the bridge's acceleration response at the midspan for different train speeds for: (a) the moving load model and (b) the moving mass model. The resonant frequencies at specific speeds for the moving load and moving mass models can be deduced by comparing the frequency spectra of the loading (Figure 2) to that of the acceleration response of the bridge given in Figure 5. In Figure 5, the effect of the loading frequencies is visible in the response of the bridge as diagonal lines crossing the FAS for both moving mass and moving

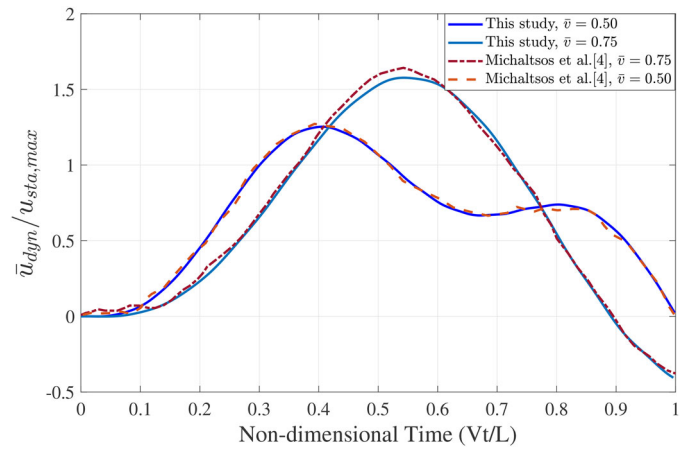


Figure 4. Ratio of the dynamic mid-span deflection to the maximum static deflection versus load position, comparison with Michaltsos et al. (1996).

$\bar{v} = 0.75$ , are presented. The normalized speed parameter  $\bar{v}$  is given by:

$$\bar{v} = \frac{2V}{\Pi} \sqrt{mL^2/EI} \quad (7)$$

Figure 4 clearly shows that the developed software is capable of estimating the dynamic behavior of a simply supported beam under a single moving mass with sufficient accuracy.

## 5. Benchmark analysis

Numerical model of the benchmark bridge was created in the developed software and both moving load and moving mass analysis under the benchmark train were carried out. Damping of the bridge was modeled using Rayleigh damping anchored at the first and fourth vertical mode frequencies. The damping ratio was specified as 2%. The boundary conditions of the bridge are defined as pinned support at one end and roller support at the other end of the bridge. The train is assumed to start its translation from the origin located at the left end of the bridge ( $x=0$ ) and continue with a constant speed during the analysis. The analysis continues approximately 40 seconds after the last axle leaves the bridge to ensure that the bridge vibrations are completely damped out.

The dynamic response of the benchmark bridge to the vibrations generated by the benchmark train under different speeds, and the sensitivity of this response to the moving speeds, are investigated by running both models for train speeds varying from 50 km/h to 350 km/h. Figure 5 shows the Fourier amplitude spectra of the bridge's acceleration response at the midspan for different train speeds for: (a) the moving load model and (b) the moving mass model. The resonant frequencies at specific speeds for the moving load and moving mass models can be deduced by comparing the frequency spectra of the loading (Figure 2) to that of the acceleration response of the bridge given in Figure 5. In Figure 5, the effect of the loading frequencies is visible in the response of the bridge as diagonal lines crossing the FAS for both moving mass and moving

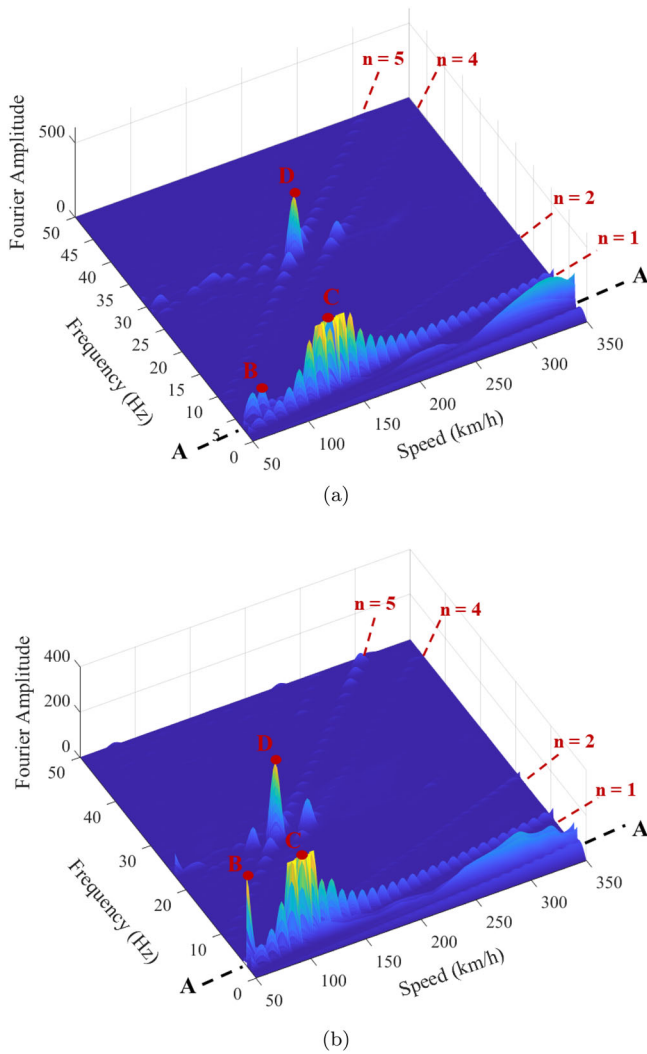


Figure 5. Frequency amplitude spectra of the acceleration responses with changing speeds (a) Moving Load model; (b) Moving Mass model.

load models. These diagonal lines are the same lines that are visible on the FAS of the loading function presented in Figure 2(a), as the loading frequencies dominate the acceleration response of the bridge at these frequencies.

Figure 5(a) and (b) also demonstrate the dominant natural frequencies of the bridge-train system, which can be identified by the lines parallel to the x-axis (speed), *i.e.*, at a constant frequency equal to the natural frequency of the bridge. For example, the dashed line A-A represents the first modal frequency of the bridge (or bridge-train system). The highest bridge response is observed at the intersection points of the diagonal lines which form at the dominant loading frequencies, and the lines parallel to the x-axis forming at the natural frequencies of the bridge. The resonance between these two frequencies causes the highest amplitudes.

While the lines representing the loading frequencies are the same for both moving load and moving mass models (the diagonal lines in Figure 5(a) and (b)), the lines representing the bridge frequencies (dashed line A-A) is shifted for these two models due to the impact of the train mass on the dominant vibration frequency of the bridge, which is

considered only in the moving mass model. Therefore, the resonance between the bridge and the loading frequencies are observed at different speeds for the moving mass and moving load model. The most visible example of this can be seen at the frequencies of 2.70 Hz and 3.50 Hz for the moving mass and moving load models, respectively. For the moving load model, the train loading causes a very high response at the first natural frequency of the bridge,  $f = 3.50\text{Hz}$ , at a speed of 130 km/h because the loading frequency at this speed is also 3.50 Hz, resulting in a resonance between the response and the loading frequencies. This phenomenon is indicated with Point C in Figure 5(a). On the other hand, for the moving mass model, this resonance occurs at a speed of 100 km/h instead of 130 km/h, which corresponds to a loading frequency of 2.70 Hz, *i.e.*, at the frequency of the train-bridge system when the train is on the bridge; see Point C in Figure 5(b). It should be noted that the Fourier amplitude at these points reaches as high as 2500 for both cases. Nonetheless, the Fourier amplitude values are truncated at 400 in Figure 5 to see the details at other frequencies and speeds.

Points B and D in Figure 5(a) and (b) represent the resonance between response and loading frequencies at the higher modes. The peak at Point B occurs due to the overlap of the second mode of the loading frequency ( $n=2$  in Equation (2)) and the first natural frequency of the bridge. The peak at Point D, on the other hand, is the result of the resonance between the fifth loading frequency ( $n=5$  in Equation (2)) and the fourth natural frequency of the bridge.

High amplitudes on the A-A line for higher train speeds than 250 km/h are observed due to the free vibration response of the structure. Also, the reader should beware that the amplitude of the FAS at resonance is proportional to the train length. For a short train, the figures could be significantly different and present several peaks.

## 6. Parametric study

After exploring the dynamic response of the benchmark bridge to the benchmark train, the study is expanded through parametric, non-dimensional analyses in order to study the impact of different parameters on the dynamic response of the railway bridges due to the vibrations induced by heavy-haul trains. The parametric study has been repeated for moving load and moving mass models and, as such, enables separate evaluation of the interaction of different parameters with the two models considered in the study. The parameters that were considered are the the span length of the bridge, bending stiffness of the bridge deck, normalized train mass and normalized train length. The impact of each of these parameters on the dynamic response of the the bridge for moving load and moving mass models was investigated for train speeds varying between 20 km/h and 360 km/h. The following subsections summarize the observations from the parametric study.

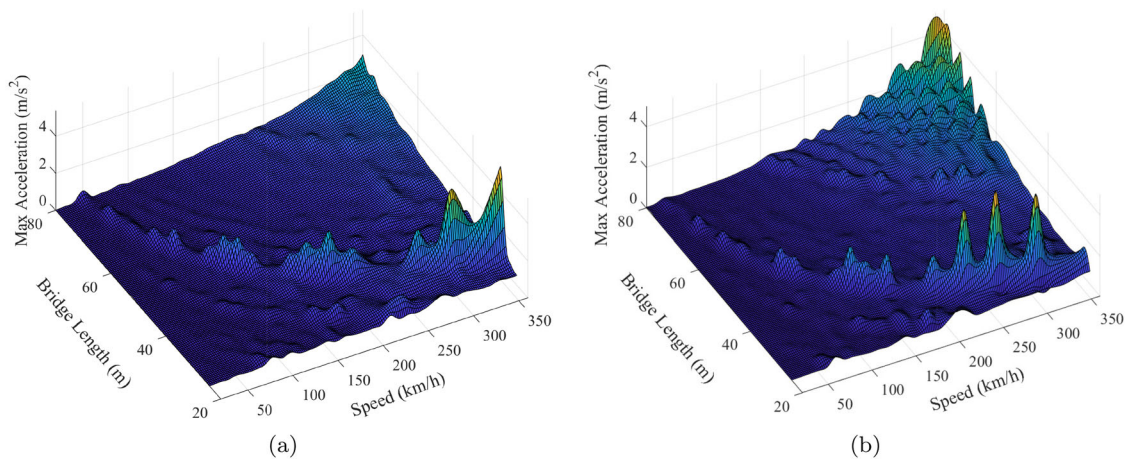


Figure 6. Variation of maximum acceleration with bridge span length and train speed for a normalized train mass of 0.76 for (a) moving load model (b) moving mass model.

### 6.1. Bridge span length

The span length of the bridge is a significant parameter in the dynamic interaction between the train and the bridge as it significantly influences the stiffness and, consequently, the natural frequencies of the bridge. Figure 6 presents the variation of maximum accelerations with the span length of a single-span bridge and the train speed computed using (a) moving load and (b) moving mass models. The maximum accelerations induced by the benchmark iron-ore train traveling at different speeds were computed at the middle of the single span for both models. In both figures, the resonance regions where the natural frequencies of the bridge and the loading frequencies of the train coincide are clearly visible through the amplified accelerations. These regions separate themselves from the rest of the plot as a series of peaks in the surface plot. These peaks follow a polynomial form as the bridge's natural frequency has a nonlinear relationship with the span length while the loading frequency has a linear relationship with the train speed.

Of the three visible resonance regions, the one that corresponds to the first vibration frequency of the bridge is the most predominant and creates several peaks along its path. The highest accelerations are observed at the short span length - high speed combination along this path. Although the two figures look pretty similar, careful inspection shows the differences in the amplification of the accelerations due to the resonance between the natural frequency of the bridge and the loading frequency. The amplification region associated with the resonance between the bridge's first vibration frequency and the loading frequency of the train is shifted for the moving mass model compared to the moving load model due to the impact of the train mass on the dominant vibration frequency.

This shift can be observed more clearly in Figure 7, where the acceleration response from both moving load and moving mass models is plotted together. The shift in the acceleration response at the resonance frequency due to the impact of the train mass is evident. For a given span length of the bridge, the resonance occurs for lower train speeds

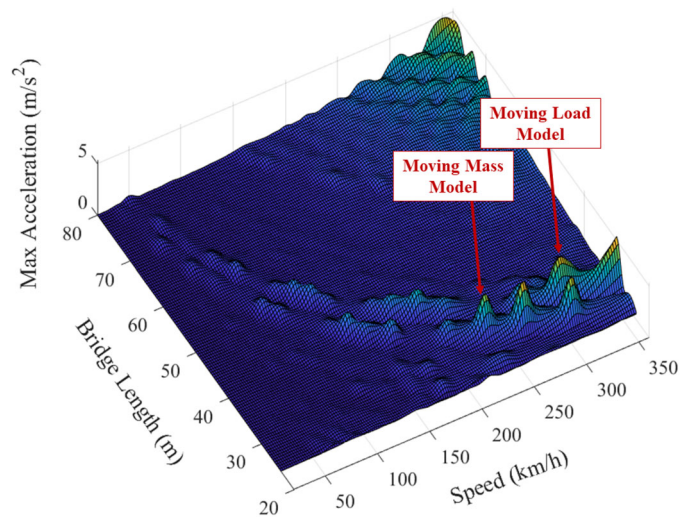


Figure 7. Effect of moving load and moving mass analysis on the maximum acceleration with varying span length and speed.

for the moving mass model compared to the moving load model because including the train mass in the analysis leads to a decrease in the natural vibration frequency. Another region of the graph where the acceleration levels are higher compared to the other regions is the long span length - high train speed region. Although the accelerations computed using the moving load model are also relatively higher for this region, the moving mass model leads to even higher accelerations for this combination; Figure 6(a) and (b).

Similar observations can also be made for the maximum displacement demand at the middle of the span, displayed in Figure 8. However, the variations in the displacement are much more subtle compared to those in the accelerations. This is because the displacement demands are mainly dominated by the dead load of the train. Although it is possible to observe the impact of resonance in the acceleration response for several modes, only the impact of the resonance in the first mode is distinctly visible for the displacement response. Furthermore, the amplification in the maximum displacement in this resonance region is much smaller compared to the amplification in the maximum accelerations. The long span length - high train speed region



again sees an amplification in the maximum displacements compared to the other regions, which is observable via the warp at the Northern corner of the otherwise relatively flat surface plotted in Figure 8.

## 6.2. Deck stiffness

Similar to the bridge span length, the deck stiffness impacts the bridge's natural frequency, affecting the dynamic interaction between the bridge and the train. This section explores the effect of the variations in the deck stiffness on the dynamic response of railway bridges induced by heavy-haul trains. For this, moving load and moving mass analyses were conducted for various train speeds and deck stiffness changing from 0.4 to 1.2 times the deck stiffness of the benchmark bridge. The benchmark train was used in all the analysis.

Figure 9 presents the maximum accelerations computed at the mid-span for different deck stiffness and train speed combinations for both moving mass and moving load models. The resonance between the first natural frequency of the bridge and the loading frequency at a given speed creates peaks in the acceleration response that is clearly visible for both models. An increase in the deck stiffness leads to an

increase in the first natural vibration frequency of the system. Therefore, the amplification in the accelerations due to the resonance between the bridge frequency and the loading frequency occurs at higher speeds for higher deck stiffness, whereas the critical train speed decreases with a decrease in the deck stiffness. In contrast to the span length, which has a non-linear relationship with the natural frequency of the bridge, the natural frequency changes linearly with the deck stiffness. Therefore, the natural frequency of the bridge and its interaction with the train speed is visible in Figure 9(a) and (b) in the form of peaks that follow a straight line.

Another region where the accelerations are amplified, especially for the moving mass model, is observed for the combination of the lowest deck stiffness and the highest train speed. This behavior is similar to that observed for long span length - high train speed combination; see Figure 6(b). Common in both cases is the high loading frequency and low bridge stiffness combination. The reason for these amplifications in the acceleration response is investigated in the next section.

## 6.3. Dynamic response of bridges with low natural frequency to high loading frequency

Figures 6 and 9 are carefully inspected by examining each peak in the low bridge frequency - high loading frequency region. The low bridge frequency is characterized by long span length in Figure 6 and by low deck stiffness in Figure 9 while the high loading frequency is characterized by high train speeds. Figure 10, which is an annotated version of the 6(b), along with two distinct reasons help to explain the complex behavior observed in this region.

The first phenomenon is related to the resonance of the higher structural modal frequencies and loading frequencies. Resonance of the loading frequency and the first modal frequency is marked in Figure 10. Also marked in Figure 10 is the resonance at second and third natural mode frequencies of the bridge. Particularly, the resonance at the third modal frequency clearly contributes to the high accelerations at lower bridge frequencies.

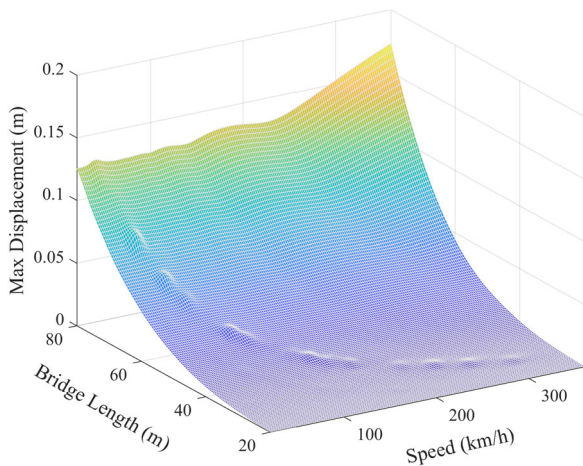


Figure 8. Variation of maximum displacement at the mid-span with bridge length and train speed for the moving mass model.

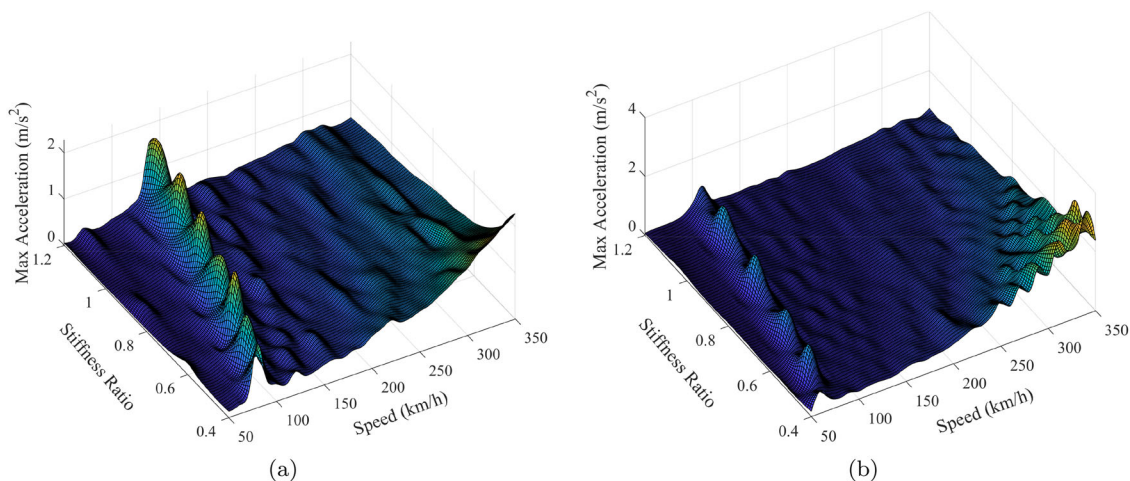


Figure 9. Variation of maximum acceleration with deck stiffness and train speed for (a) moving load model (b) moving mass model.

The final cause of the amplified response is the increase in the ratio of the forcing frequency to the natural frequency of the bridge,  $\omega/\omega_n$ . For a harmonic force, which can be assumed to represent train loading in a satisfactory manner, the acceleration response increases quadratically with an increase in the  $\omega/\omega_n$ , once  $\omega/\omega_n$  exceeds 1.5 (Chopra (2017)). Hence, as the loading frequency (train speed) increases and the bridge frequency decreases (i.e. increased bridge length in Figure 10),  $\omega/\omega_n$  value increases for both the first and the second mode of the bridge leading to an amplification in the accelerations in these modes. Consequently, the acceleration response in each of the first three modes of the bridges with low frequencies (i.e. high span length or low deck stiffness) subjected to high frequency loading is relatively high. The high accelerations in the first two modes are attributed to the relatively high  $\omega/\omega_n$  for these modes, while, for the third mode the  $\omega/\omega_n$  approaches 1.0 leading to a resonance in this mode. This leads to the high accelerations in Figures 6 and 9 for the high loading frequency, low bridge frequency regions. The

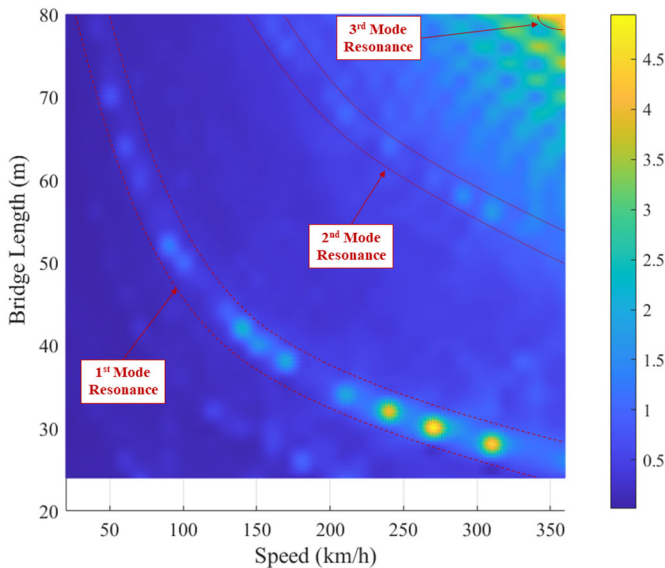


Figure 10. Variation of maximum acceleration with bridge length and train speed as contour plot.

increase in the acceleration response due to increasing train speed is also observed in comprehensive experimental (Xia et al. (2005)) and numerical (Xia and Zhang (2005)) studies.

#### 6.4. Normalized train length

Figure 11 presents the variation of maximum acceleration with the normalized train length and the train speed for (a) the moving load model and (b) for the moving mass model. In this study, the normalized train length is defined as the ratio of the total length of the train to the span length of the bridge. For the benchmark train, the normalized train length is 13.9; the total length of the benchmark train is 696.3 m while the bridge span length is 50 m. The first observation that can be deduced from Figure 11 is that the maximum accelerations at the mid-span increase rapidly as the normalized train length increases from 2.0 up to 6.0, where it saturates at a constant value for both the moving load and moving mass models. This observation indicates that the impact of repetitive loads in the accelerations on the bridge is significant to a certain extent. The additional loads when the normalized length of the train exceeds 6.0 do not provide any further amplification in the maximum accelerations.

Unlike the other parameters considered in this study, the normalized train length does not impact the natural frequency of the system. Therefore the resonance characteristics of the moving mass and moving load models of the benchmark bridge under the benchmark train loading summarized in section 2 remains the same for different train lengths.

#### 6.5. Normalized train mass

The train mass has two potential impacts on the dynamic interaction between heavy-haul trains and railway bridges. First, the train mass creates the dynamic loading on the bridge and, as such, directly impacts the dynamic behavior for both moving load and moving mass models. Second, the train mass, when modeled as a moving mass, affects the natural vibration frequency of the bridge, potentially leading to a variation in its dynamic behavior. In this study, the

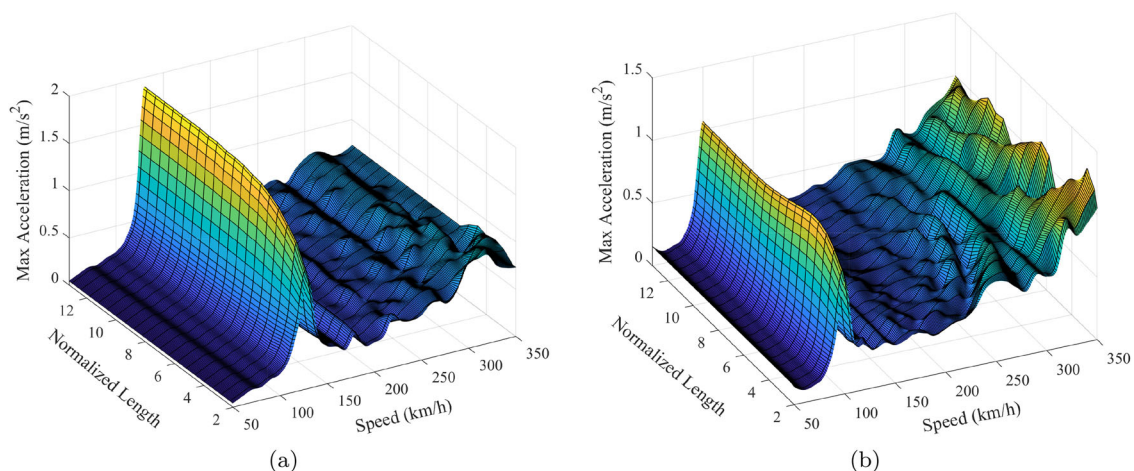


Figure 11. Variation of maximum acceleration with normalized train length and speed of the Train for a normalized train mass of 0.76 for (a) moving load model (b) moving mass model.

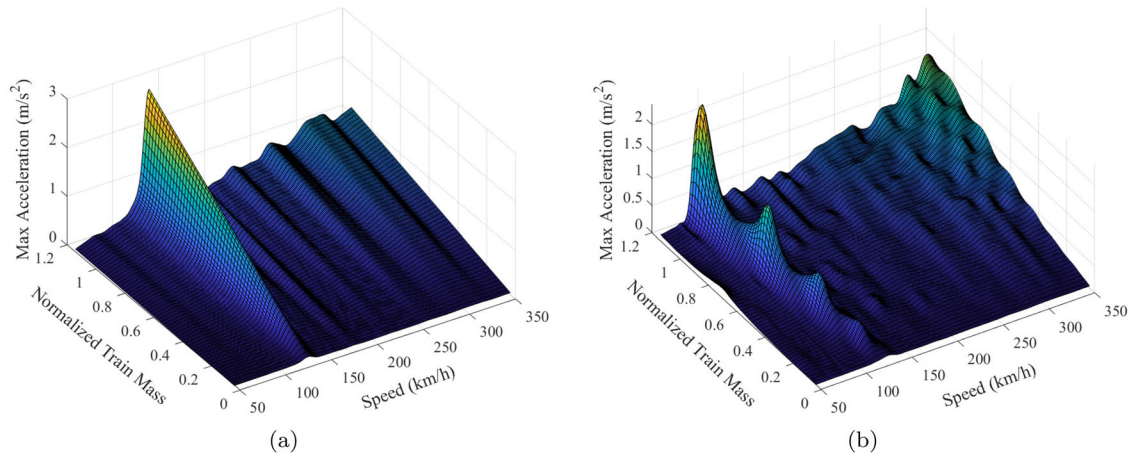


Figure 12. Variation of maximum acceleration with train mass and train speed for (a) moving load model (b) moving mass model.

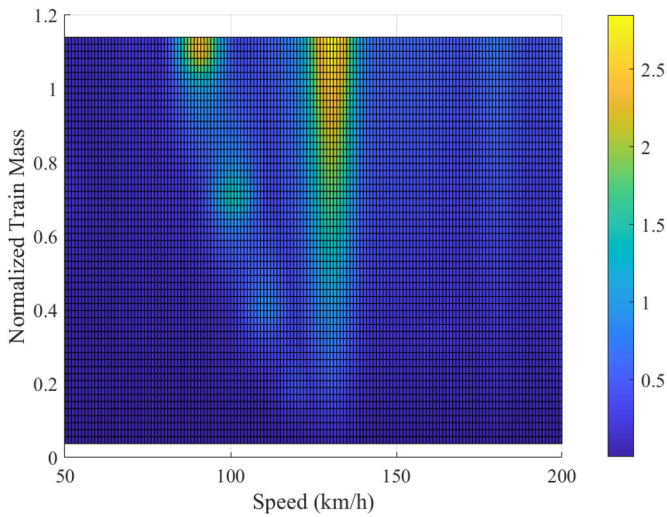


Figure 13. Effect of the train mass on the maximum acceleration demands for moving load and moving mass models plotted together.

variability of the train mass with respect to the mass of the bridge is represented by the normalized train mass, which is defined as the ratio of the maximum train mass that is on the bridge at a given instant to the mass of the bridge itself; see section 2 for the detailed definition of the normalized train mass. In order to explore the effect of the train mass on the dynamic behavior of the bridge, the normalized train mass parameter is varied between 0.1 and 1.2 by changing the axle load while keeping all other variables constant.

Figure 12 shows the variation of maximum accelerations at the mid-span with normalized train mass and train speed obtained using (a) moving load and (b) moving mass models. The impact of resonance between the first natural frequency of the bridge and the loading frequency can be seen from the figure for both models. For the moving load model, the accelerations increase linearly with train mass due to the increased axle loads at the resonance speed, which is constant since the natural frequency of the bridge does not vary for this model; Figure 12(a).

On the other hand, the increased train mass has a more complex impact on the critical speed and the maximum acceleration demands for the moving mass model (Figure 12(b)) compared to the moving load model. The maximum

accelerations at the resonance frequency follow a nonlinear path between the peaks observed at normalized mass values of 0.42, 0.70, and 1.12. Furthermore, while the critical speed remains constant for the moving load model, it changes with train mass for the moving mass model. This can also be observed in the contour plot in Figure 13, where the maximum accelerations are plotted for both the moving load model and the moving mass model for train speeds between 50 km/h and 200 km/h. For the moving load model, the critical speed remains constant at 130 km/h, as the natural frequency of the bridge remains constant with varying train mass. On the other hand, for the moving mass model, the critical speed is also observed to be approximately 130 km/h for cases where the normalized train mass is less than 0.4. For such low values, the train mass does not significantly impact the natural frequency of the bridge and, therefore, the critical speed remains virtually equal to that for the moving mass model. However, with the increase in the normalized train mass beyond the threshold value of 0.4, the natural frequency of the moving mass model reduces significantly due to the mass of the train leading to lower critical speeds.

### 6.6. Amplifications in accelerations due to inertia of the train

As summarized in Section 6.5, the mass of the train significantly impacts the maximum accelerations observed on the bridge. When the loading frequency is close to the vibration frequency of the bridge itself, the moving load model provides conservative results compared to the moving mass model as far as the amplitude of the maximum accelerations is concerned. However, when the loading frequency is close to the vibration frequency of the bridge with the additional mass of the train, the moving load model can significantly underestimate the maximum accelerations leading to non-conservative estimates. This might have severe implications for the speed limits set for the trains. In this section, the amplification in the accelerations due to the influence of including the train mass in the analysis will be investigated. For this, a new parameter named acceleration amplification factor (AAF), defined as the ratio of the maximum acceleration at the middle of the bridge span computed from the

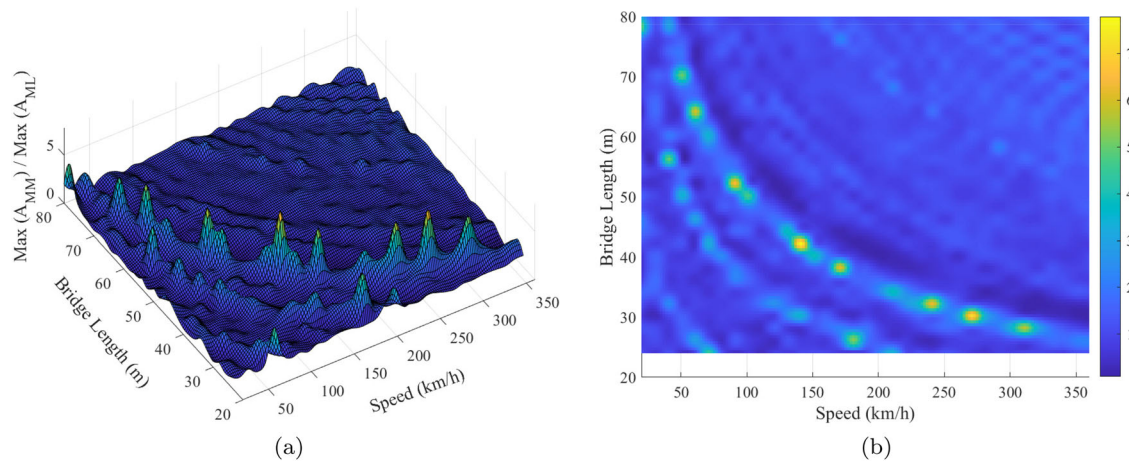


Figure 14. Variation of Acceleration Amplification Factor with bridge length and speed of the train for a normalized train mass of 0.76 in (a) 3 D and (b) 2 D representation.

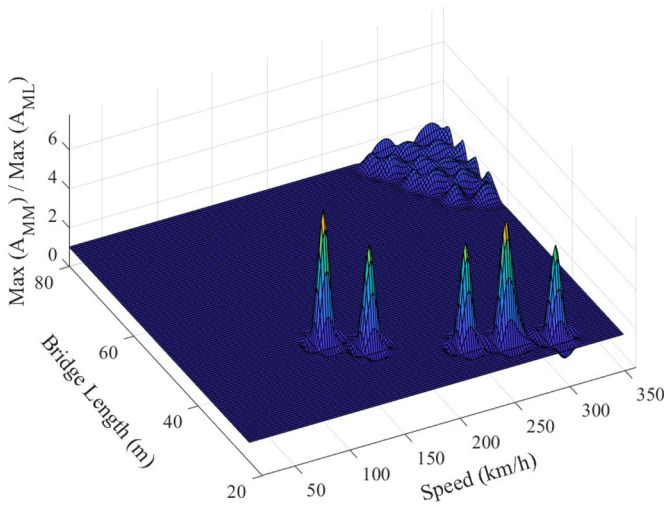


Figure 15. Variation of AAF with bridge length and train speed for a normalized train mass of 0.76; the maximum acceleration from the moving mass analysis is greater than  $2.0 \text{ m/s}^2$ .

moving mass model to that obtained from the moving load model, is introduced.

Figure 14 shows the variation of the acceleration amplification factor with bridge length and train speed for a normalized train mass of 0.76. Figure 14 (a) and (b) present essentially the same data; the former shows more detailed information about the variation of the acceleration amplification factor. The latter clearly shows the path the highest peaks of the acceleration amplification factor follow in the bridge length – train speed surface plot in plan view. The peaks in the acceleration amplification factor occur where the natural frequency of the moving mass model and the loading frequency lead to a resonance.

As shown earlier, the natural frequency of the moving load model is considerably higher compared to that of the moving mass model. As such, at certain loading frequencies, the natural frequency of the moving mass model matches that of the loading while the natural frequency of the moving load model does not. This leads to the peaks in the amplification factor shown in Figure 14(a). Figure 14(b) depicts the relationship between the frequency of the bridge including the mass of the

train, which varies non-linearly with the bridge length, and the loading frequency, which varies linearly with the train speed. As a result, the peaks in the acceleration amplification factor follow a nonlinear path. Although Figure 14(a) shows several peaks, some of these peaks result from dividing two relatively low values by each other. In other words, for some cases, although the maximum acceleration estimate is amplified significantly by including the train mass in the dynamic analysis, the value of the maximum acceleration itself remains relatively small, and thus, well within the requirements of the regulations for both models.

In order to eliminate those cases, Figure 14(a) is re-plotted in Figure 15, but in this case, the plot is limited to those cases where the maximum acceleration estimate from the moving mass model is at least  $2.0 \text{ m/s}^2$ . This limit is selected because the maximum acceleration limit according to EN 1991-2 (Standardization (2003)) for ballasted bridges is  $3.5 \text{ m/s}^2$  to ensure ballast stability. The value of  $2.0 \text{ m/s}^2$  is selected as the threshold here instead of  $3.5 \text{ m/s}^2$  because the maximum acceleration level starts to get close to the limit and becomes interesting for the behavior of the bridge. The difference between Figures 14(a) and 15 shows that the amplification in the maximum acceleration due to the mass of the train becomes essential for certain bridge length – train speed combinations.

Most of these combinations are short-span, high-speed combinations. Two of the combinations out of this range are for the span lengths of 38 m and 42 m. When combined with a train speed of 170 km/h and 140 km/h, the acceleration amplification factor for these span lengths is 7.8 and 6.2, respectively. In other words, for these span length – train speed combinations, the maximum accelerations computed using a moving mass model are 780% and 620% higher than those computed using a moving load model. These two combinations can be of significant importance as trains with relatively high mass are more likely to travel at these speeds than at the higher speeds, where the other peaks in AAF are observed in Figure 15.

Finally, to explore the impact of the train mass on the variation of acceleration amplification factor, the analysis

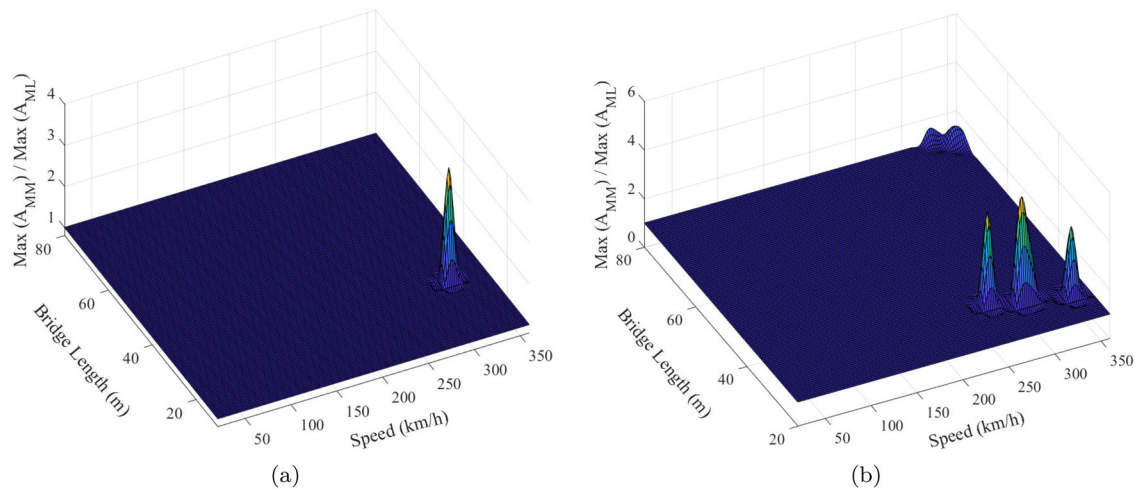


Figure 16. Variation of AAF with bridge length and train speed for a normalized train mass of (a) 0.25 and (b) 0.5.

summarized above was repeated for normalized train masses of 0.25 and 0.5. Figure 16 demonstrates that the decrease in the normalized train mass leads to a significant decrease in the acceleration amplification factors. Only the relatively high-speed region remains significantly influenced by the mass of the train for normalized train masses of 0.25 and 0.5. However, it should be noted that, unlike the normalized train mass of 0.76, the speeds of 250 km/h and higher cannot necessarily be deemed very high for the relatively lower train masses of 0.25 and 0.5. The high-speed train and short-span bridge combinations are prevalent and Figure 16 indicate that the critical speed and the acceleration response might be significantly different when the train's mass is included in the analysis.

## 7. Conclusions

Ever-increasing demands on railway bridges necessitate their safety assessment for higher train speeds and axle loads. The scarcity of research investigating the dynamic behavior of railway bridges under vibrations induced by heavy-haul trains and the effects of crucial model parameters on this behavior motivated this study.

A Finite Element code that can take the inertial effects of the train mass into account is generated to analyze the behavior of simply-supported railway bridges. The code is then verified using the existing literature.

Norrdals Bridge in Norway that carry heavy-haul iron ore trains with axle loads up to 325 kN and a typical freight train that crosses this bridge are considered as the benchmark case. Further, a parametric study is conducted to investigate the impact of different parameters on the dynamic behavior of the bridge: span length of the bridge, normalized train length, normalized train mass, and deck stiffness. For this, dynamic analysis using moving load and moving mass models for a range of the given parameters was conducted for different train speeds. Finally, a new parameter, acceleration amplification factor (AAF), is defined to quantify the effect of the inertia of the train on the bridge response at different train speeds. As a result of the

extensive numerical analysis conducted, the following conclusions were drawn.

- Comparing the acceleration response of the benchmark bridge computed using moving load and moving mass models under the loading from the benchmark train highlighted the significance of the train mass on the natural frequency of vibration. Due to the relatively high mass of the benchmark train, the natural frequency of vibration varied as much as 25% between the moving load and moving mass models. This difference in the natural vibration frequencies lead to a shift in the critical train speed, i.e., the speed where the loading and vibration frequencies match and result in resonance.
- Bridge span length directly impacts the natural frequency of vibration for both moving mass and moving load models. As such, for both models, the critical speed, where the loading and response frequencies match, is significantly impacted by the bridge length. For a given bridge length, moving load model overestimates the critical speed compared to the moving mass model because of the shift in the natural vibration frequency of the bridge due to the train mass considered in the latter model.
- The bending stiffness of the deck affects the dynamic behavior of the bridge similar to the bridge span length for both moving mass and moving load models. The main difference between the bridge span length and the deck stiffness is the order of magnitude of the impact: The deck stiffness impacts the overall stiffness and the vibration frequency of the bridge linearly, while the impact of the bridge span length is nonlinear.
- For both bridge span length and deck stiffness parameters, the maximum accelerations are mainly observed for the regions where the vibration and loading frequencies match each other. However, particularly for the moving mass model, relatively high accelerations are also observed for the region where the vibration frequency of the bridge is low and the loading frequency is high; i.e. low deck stiffness (or long bridge span) and high train speed combination.

- Unlike the other parameters considered in this study, the normalized train length does not impact the natural vibration frequency of the bridge. Therefore, the critical speed and the resonance behavior of the bridge is not impacted by the normalized train length. However, the accelerations created by shorter trains are lower compared to those created by their longer counterparts. The accelerations increase linearly between the normalized train lengths of 2 and 6 highlighting the impact of repetitive loads. When the normalized train length exceeds 6, this impact saturates and the acceleration demands does not increase further for longer train lengths.
- The train mass has a two-fold impact on the dynamic behavior of the bridge. First, the axle load is imposed on the bridge as dynamic load and it directly impacts the bridge's behavior. For the moving load model, it is indicated by a linear increase in the acceleration demands with the train mass. Secondly, for the moving mass model, the vibration frequency is significantly impacted by the train mass. This effect can be stated to be insignificant when the normalized train mass remains below 0.4. However, when this threshold is exceeded, the vibration frequency of the bridge is impacted significantly leading to a shift in the critical train speed that creates resonance in the bridge response.
- The ratio of the maximum accelerations obtained from moving mass and moving load models, AAF, was observed to be at its highest where the loading frequency matches the natural frequency of the moving mass system. In such cases, the acceleration demands are amplified due to the resonance. On the other hand, the moving load model has a significantly different natural frequency than the moving mass model and, thus, leads to much lower acceleration demands at this frequency leading to very high acceleration amplification factors. These amplifications in the acceleration demands are highest for a normalized mass ratio of 0.76 and decreases with a decrease in the train mass.

This study contributes to understanding the dynamic behavior of railway bridges trafficked by heavy-haul trains. The parametric study and three-dimensional presentations of the response parameter, train speed, and the variable parameter depicts a clear picture of the amplification in the acceleration response due to the loading frequency (train speed) and bridge properties. The outcomes of this study demonstrates the importance of including the train mass in the analysis, especially when the train mass is significant compared to that of the bridge.

The study is limited to simply-supported bridges and a single train geometry. Further research is necessary to expand the observations made in this study to multi-span bridges and different train geometries. Finally, a moving system model that considers the stiffness and damping properties of the train shall be incorporated in the future studies to quantify the impact of these two parameters on the dynamic behavior of the railway bridges exposed to heavy axle loads.

## Disclosure statement

No potential conflict of interest was reported by the authors.

## ORCID

Emrah Erduran  <http://orcid.org/0000-0003-1486-9631>  
Semih Gonen  <http://orcid.org/0000-0002-9588-4552>

## References

- Arvidsson, T., & Karoumi, R. (2014). Train-bridge interaction – a review and discussion of key model parameters. *International Journal of Rail Transportation*, 2(3), 147–186. Retrieved from. doi: 10.1080/23248378.2014.897790
- Casas, J. R., & Moughty, J. J. (2017). Bridge damage detection based on vibration data: Past and new developments. *Frontiers in Built Environment*, 3(February), 1–12. doi:10.3389/fbuil.2017.00004
- Cheng, Y. S., Au, F. T., & Cheung, Y. K. (2001). Vibration of railway bridges under a moving train by using bridge-track-vehicle element. *Engineering Structures*, 23(12), 1597–1606. doi:10.1016/S0141-0296(01)00058-X
- Chopra, A. K. (2017). *Dynamics of structures* (5th ed.). Essex, England: Pearson Education Limited.
- Doménech, A., Museros, P., & Martínez-Rodrigo, M. D. (2014). Influence of the vehicle model on the prediction of the maximum bending response of simply-supported bridges under high-speed railway traffic. *Engineering Structures*, 72, 123–139. doi:10.1016/j.engstruct.2014.04.037
- Fryba, L. (1999). *Vibration of solids and structures under moving loads*. Netherlands: Springer.
- Garinei, A., & Risitano, G. (2008). Vibrations of railway bridges for high speed trains under moving loads varying in time. *Engineering Structures*, 30(3), 724–732. doi:10.1016/j.engstruct.2007.05.009
- Ichikawa, M., Miyakawa, Y., & Matsuda, A. (2000). Vibration analysis of the continuous beam subjected to a moving mass. *Journal of Sound and Vibration*, 230(3), 493–506. doi:10.1006/jsvi.1999.2625
- Jin, Z., Li, G., Pei, S., & Liu, H. (2017). Vehicle-induced random vibration of railway bridges: a spectral approach. *International Journal of Rail Transportation*, 5(4), 191–212. doi:10.1080/23248378.2017.1338538
- Ju, S. H., & Lin, H. T. (2003). Resonance characteristics of high-speed trains passing simply supported bridges. *Journal of Sound and Vibration*, 267(5), 1127–1141. doi:10.1016/S0022-460X(02)01463-3
- Ju, S. H., Lin, H. T., & Huang, J. Y. (2009). Dominant frequencies of train-induced vibrations. *Journal of Sound and Vibration*, 319(1-2), 247–259. doi:10.1016/j.jsv.2008.05.029
- Karoumi, R. (1998). *Response of cable-stayed and suspension bridges to moving vehicles*. Doctoral Thesis, KTH Royal Institute of Technology, Stockholm.
- Kwark, J. W., Choi, E. S., Kim, Y. J., Kim, B. S., & Kim, S. I. (2004). Dynamic behavior of two-span continuous concrete bridges under moving high-speed train. *Computers & Structures*, 82(4–5), 463–474. doi:10.1016/S0045-7949(03)00054-3
- Liu, K., De Roeck, G., & Lombaert, G. (2009). The effect of dynamic train-bridge interaction on the bridge response during a train passage. *Journal of Sound and Vibration*, 325(1-2), 240–251. doi:10.1016/j.jsv.2009.03.021
- Lu, Y., Mao, L., & Woodward, P. (2012). Frequency characteristics of railway bridge response to moving trains with consideration of train mass. *Engineering Structures*, 42, 9–22. doi:10.1016/j.engstruct.2012.04.007
- Majka, M., & Hartnett, M. (2008). Effects of speed, load and damping on the dynamic response of railway bridges and vehicles. *Computers & Structures*, 86(6), 556–572. doi:10.1016/j.compstruc.2007.05.002
- Michaltsos, G., Sophianopoulos, D., & Kounadis, A. N. (1996). The effect of a moving mass and other parameters on the dynamic response of a simply supported beam. *Journal of Sound and Vibration*, 191(3), 357–362. doi:10.1006/jsvi.1996.0127

- Salehi, M., Demirlioglu, K., & Erduran, E. (2021). Evaluation of the effect of operational modal analysis algorithms on identified modal parameters of railway bridges. Proceedings of the IABSE Congress - Structural Engineering for Future Societal Needs, Zurich, Switzerland. doi:10.2749/ghent.2021.0441
- Standardization, E. C. (2003). *EN 1991-2 Eurocode 1: Actions on structures - Part 2: Traffic loads on bridges*. Brussels: CEN.
- Wiberg, J. (2009). Railway bridge response to passing trains: Measurements and FE model updating. Doctoral Thesis, KTH Royal Institute of Technology, Stockholm.
- Xiao, Y., Luo, X., Liu, J., & Wang, K. (2020). Dynamic response of railway bridges under heavy-haul freight trains. *Advances in Civil Engineering*, 2020, 1–13. doi:10.1155/2020/7486904
- Xia, H., & Zhang, N. (2005). Dynamic analysis of railway bridge under high-speed trains. *Computers & Structures*, 83(23–24), 1891–1901. doi:10.1016/j.compstruc.2005.02.014
- Xia, H., Zhang, N., & Gao, R. (2005). Experimental analysis of railway bridge under high-speed trains. *Journal of Sound and Vibration*, 282(1–2), 517–528. doi:10.1016/j.jsv.2004.04.033
- Xia, H., Zhang, N., & Guo, W. (2006). Analysis of resonance mechanism and conditions of train-bridge system. *Journal of Sound and Vibration*, 297(3–5), 810–822. doi:10.1016/j.jsv.2006.04.022
- Yang, Y. B., & Lin, C. W. (2005). Vehicle-bridge interaction dynamics and potential applications. *Journal of Sound and Vibration*, 284(1–2), 205–226. doi:10.1016/j.jsv.2004.06.032
- Yang, Y. B., Lin, C. L., Yau, J. D., & Chang, D. W. (2004). Mechanism of resonance and cancellation for train-induced vibrations on bridges with elastic bearings. *Journal of Sound and Vibration*, 269(1–2), 345–360. doi:10.1016/S0022-460X(03)00123-8
- Zhu, Z., Wang, L., Yu, Z., Gong, W., & Bai, Y. (2018). Non-stationary random vibration analysis of railway bridges under moving heavy-haul trains. *International Journal of Structural Stability and Dynamics*, 18(3), 1850035. doi:10.1142/S0219455418500359